IET Microwaves, Antennas & Propagation

Research Article

Low profile and wideband planar inverted-F antenna with polarisation and pattern diversities

ISSN 1751-8725
Received on 23rd May 2015
Revised on 2nd August 2015
Accepted on 29th August 2015
doi: 10.1049/iet-map.2015.0337
www.ietdl.org

Saqer Al Ja'afreh ✉, *Yi Huang*, *Lei Xing*

Department of Electrical Engineering and Electronics, University of Liverpool, L69 3GJ, Liverpool, UK
✉ *E-mail: s.al-jaafreh@liverpool.ac.uk*

Abstract: A low profile (height = 3 mm) and wideband dual coplanar feed planar inverted-F antenna (PIFA) is proposed for diversity applications over the frequency range of 2.35–3.25 GHz with a fractional bandwidth of 32%. It covers LTE bands 7, 38, 40, 41 and WiFi frequency bands. The design is based on a comparative study on the mutual coupling between different feed arrangements such as the parallel feed, coplanar feed and orthogonal feed. The results show that the coplanar feed arrangement exhibits a lower mutual coupling level. As a result, the coplanar feed is employed in the proposed antenna and the polarisation diversity is achieved by exciting two orthogonal radiation modes; the antenna fed by Feed 1 uses open ground plane slot in the horizontal plane, while the antenna fed by Feed 2 is linked to PIFA. The modified top plate provides a self-matching circuit for Feed 2. The isolation between the feeds is achieved by an L-shaped ground plane slot. Both simulated and measured results are obtained, and the results demonstrate that the proposed antenna is a very good candidate for mobile diversity and multiple-input and multiple-output applications.

1 Introduction

Nowadays, there is a strong demand for a higher data rate and better reliability in wireless communication systems. The multiple-input and multiple-output (MIMO) technology [1] has become a core technology to meet this demand. This is related to its ability in increasing the channel capacity with the number of antennas at both communication ends without using the conventional techniques such as increasing transmitted power or using more spectrum [2]. Moreover with multiple antenna schemes, the antenna diversity plays an important role in increasing the reliability of wireless systems.

MIMO antenna design can be conducted normally using either multiple element antennas (MEA) or isolated mode antenna technology (IMAT). It has been shown that MEA arranged in a pattern or polarisation diversity configuration with sufficient antenna spacing can offer a large diversity gain [3]. However, recent trends in mobile market require small and slim handset terminals for multisystem – these increase the demand for low profile, small size, and multiband/wideband antennas. To meet the compactness requirement for MIMO antenna systems, IMAT was introduced as a new design approach [4] in which a single antenna element with more than one feed can be used as a compact MIMO antenna scheme. However, the compact MIMO antenna is normally achieved at the expense of a large mutual coupling level, thus isolation techniques are required.

The isolation between MIMO antenna elements or ports is a critical design parameter. Strongly coupled antennas have very poor radiation efficiency and MIMO system performance, because an antenna element or port will act as a load for the other elements or ports [5]. Up to now, several isolation techniques have been proposed to reduce the antenna mutual coupling in small portable devices. Changing the spacing of antennas is one of the oldest techniques to decrease the mutual coupling level [5], but this technique is not suitable for small portable devices because of the limited space. Matching networks have been used as decoupling networks and applied to several antenna structures such as monopoles [6] and planar inverted-F antenna (PIFAs) [7]. However this technique has several drawbacks: the first one lies in the resulted ohmic losses from the matching network components, the second issue is the large utilised space, and the third problem is that the antenna bandwidth obtained is narrow [6]. A neutralisation line with an optimised shape and dimensions provides a reverse current path of the original path between antenna elements [8, 9]. In addition, a defect ground plane structure [10, 11] is one of the popular isolation techniques and it has been widely used for closely spaced and coupled antennas.

Among various antenna structures such as monopoles, patches, and slots, the PIFA has received a lot of attention for MIMO antenna systems [11, 12]. Recently, compact dual-feed diversity PIFA antennas were proposed for MIMO applications [13–15]. Although these designs were novel, they have several drawbacks such as the height of these antennas is relatively large and the bandwidth is relatively narrow [13–15], thus it is difficult to use them in real applications.

In this paper, a new wideband and very low profile PIFA antenna with a new feed arrangement is proposed for wireless applications over the frequency range of 2.35–3.25 GHz. It employs a polarisation diversity that is achieved using a coplanar feed. The work presented in this paper can be considered as the continuation of our work reported in [13–15] in the sense of using dual-feed to form a MIMO and diversity antenna. It presents a new PIFA feed arrangement (coplanar feed) that offers excellent features to overcome the aforementioned drawbacks of other feed arrangements in [13–15], it offers a lower mutual coupling level and, at the same time it allows the use of waveguide slots to achieve the desired radiation and isolation.

This paper is organised as follows: Section 2 is about a comparative study on the mutual coupling between different feed arrangements. Section 3 presents the new design. In Section 4, the prototype, scattering parameters, current distributions and far-field radiation patterns are provided and discussed. Section 5 deals with diversity characteristics and MIMO performance of the prototype; the envelope correlation coefficient (ECC), mean effective gains (MEG), total radiation efficiency and the diversity gain of the antenna are obtained and discussed. Finally, the conclusion is drawn in Section 6.

2 Feed arrangement comparative study

Recently, three multi-port PIFA antennas were proposed [13–15]. However, they have drawbacks such as high profiles, relatively narrow bandwidths and large top plate sizes which are impractical for real applications. Here, a comparative study on the mutual coupling between PIFA feed arrangements is conducted with the aim to find a solution for the aforementioned drawbacks.

It is well-known that the mutual coupling between MEAs depends on several factors, such as element radiation pattern, array geometry or relative orientation of array elements. In this context, three PIFA feed arrangements are given in Figs. 1*a*–*c*: a coplanar feed case, a parallel feed case and an orthogonal feed case. It is worth mentioning that in these cases all parameters are the same except the feed arrangement and shorting pin positions. Fig. 1*d* shows the mutual coupling coefficients obtained using a simulation tool (CST Microwave Studio). We can see that the orthogonal feed exhibits the lowest mutual coupling level – this is obviously due to the utilisation of the polarisation diversity between the two antenna feeds. However, the coplanar is selected as the main feed

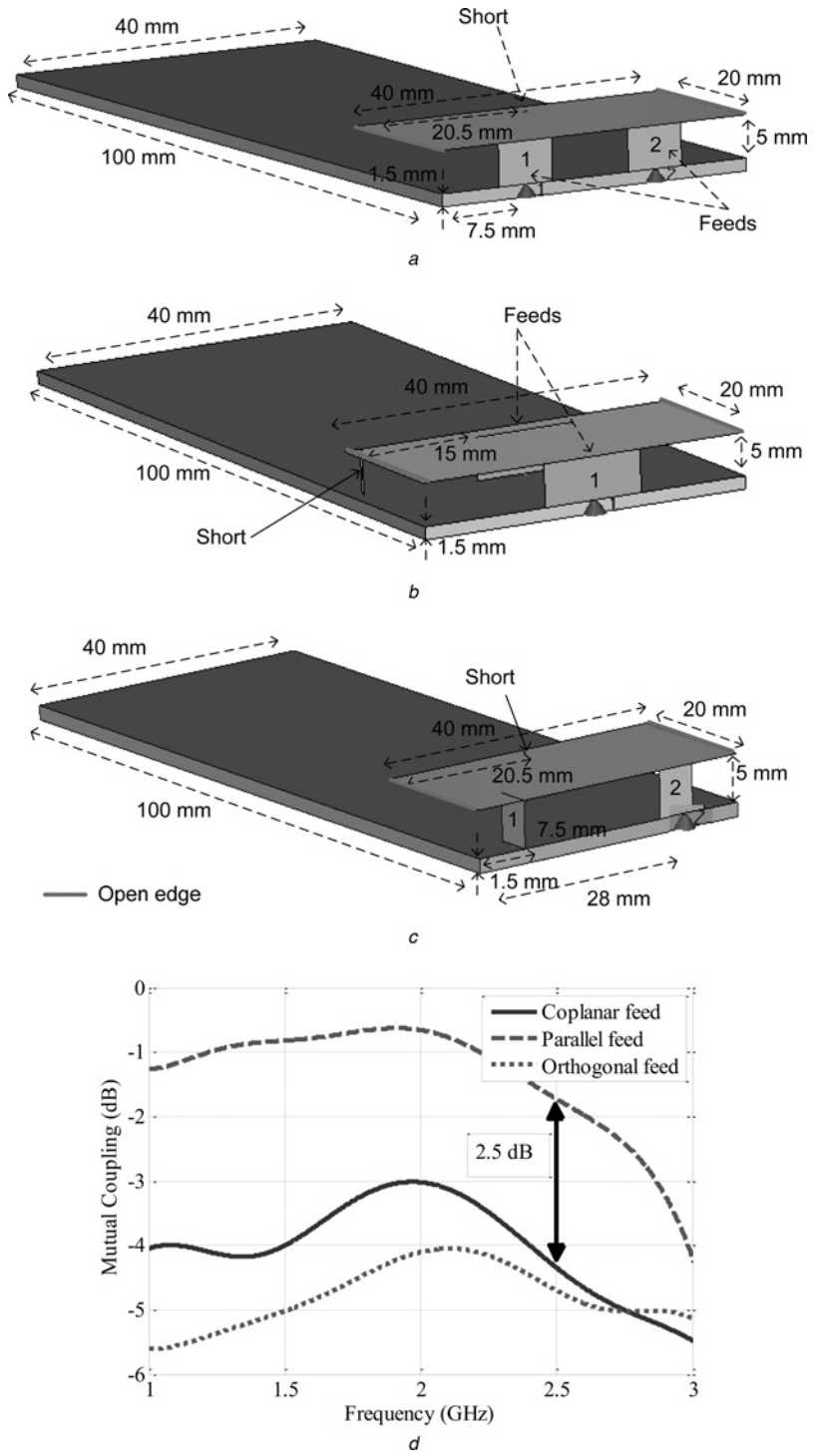

Fig. 1 *Feed arrangements comparative study*

a PIFA with coplanar feed
b PIFA with parallel feed
c PIFA with orthogonal feed
d Mutual coupling between PIFA feeds

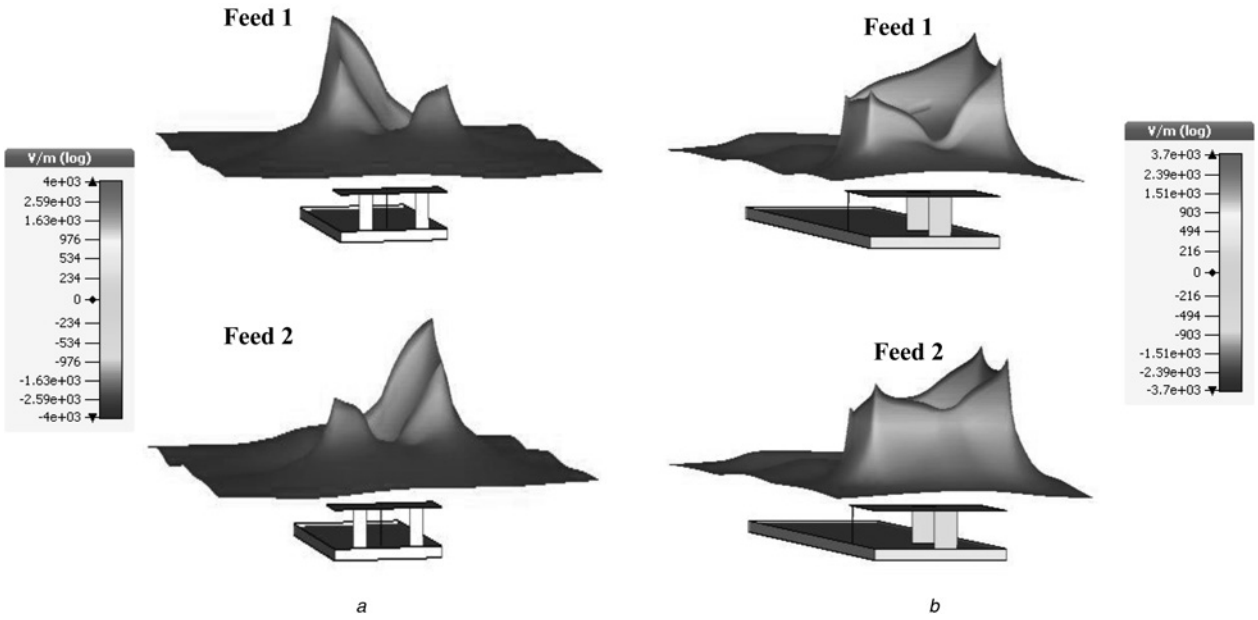

Fig. 2 *Electric field distributions on top plate*

a Coplanar feed
b Parallel feed

arrangement in this work due to the following reasons: (i) It has about 2.5 dB less mutual coupling than the parallel feed case by average. Moreover, it has a similar mutual coupling level to the orthogonal feed case for frequencies above 2.5 GHz. (ii) It is a new feed arrangement that has not been employed in previous designs of a dual-feed PIFA. (iii) It offers a geometry of a parallel plate waveguide which permits the use of slot waveguide theory to produce either radiation or isolation. From this result, we can ask two questions: why does the coplanar feed provide a smaller coupling level? and how to optimise this arrangement for MIMO applications? The answers can be found from the electric field distribution on the top plate and from the geometry of the structure with coplanar feed case, respectively.

The first issue can be explained from the electric field distribution as shown in Fig. 2. It can be seen that both feeds share the same open edge of PIFA in the case of parallel feed, while for the coplanar case, each feed has its own open edge. In other words, this means that the mutual coupling in parallel feed case has the following two sources: the near field coupling and the surface current coupling. In the case of coplanar feed, there is only one source of mutual coupling, and it is the surface current.

To deal with the second issue, it is worth noting that the surface current is the effective source of mutual coupling; this can be found from the theory of characteristic mode [16]. The chassis of size (40 mm × 100 mm) is selected as an example and it has a full wave characteristic mode around 2.5 GHz as shown in Fig. 3*a*.

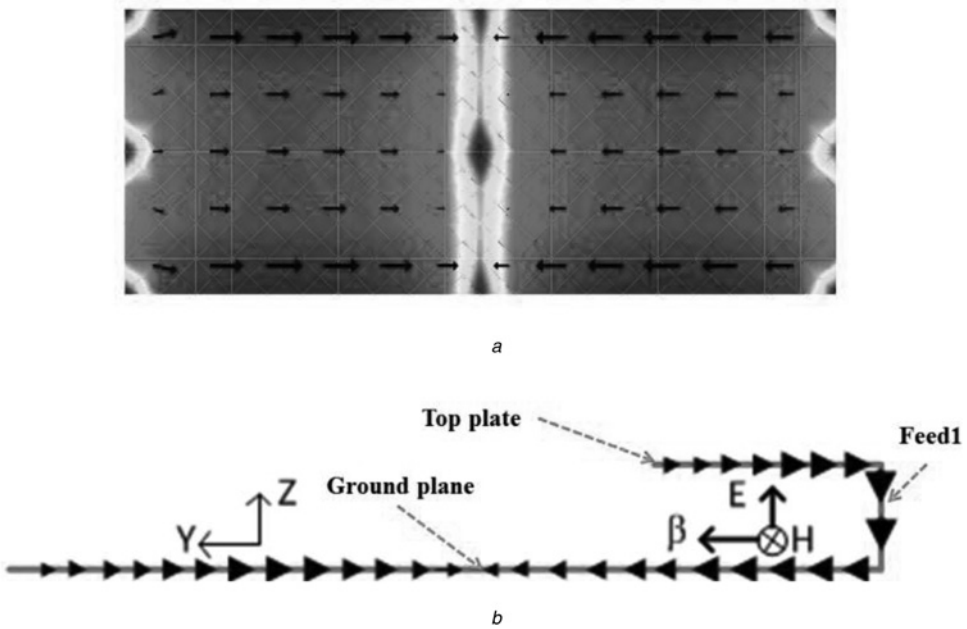

Fig. 3 *Chassis of size (40 mm × 100 mm) is selected as an example and it has a full wave characteristic mode*

a Characteristic mode of a rectangular 40 mm × 100 mm ground plane computed at 2.5 GHz [16]
b Side view of dual-coplanar-Feed PIFA over the ground plane with surface current distribution and excited fields between parallel plates

IET Microw. Antennas Propag., 2016, Vol. 10, Iss. 2, pp. 152–161

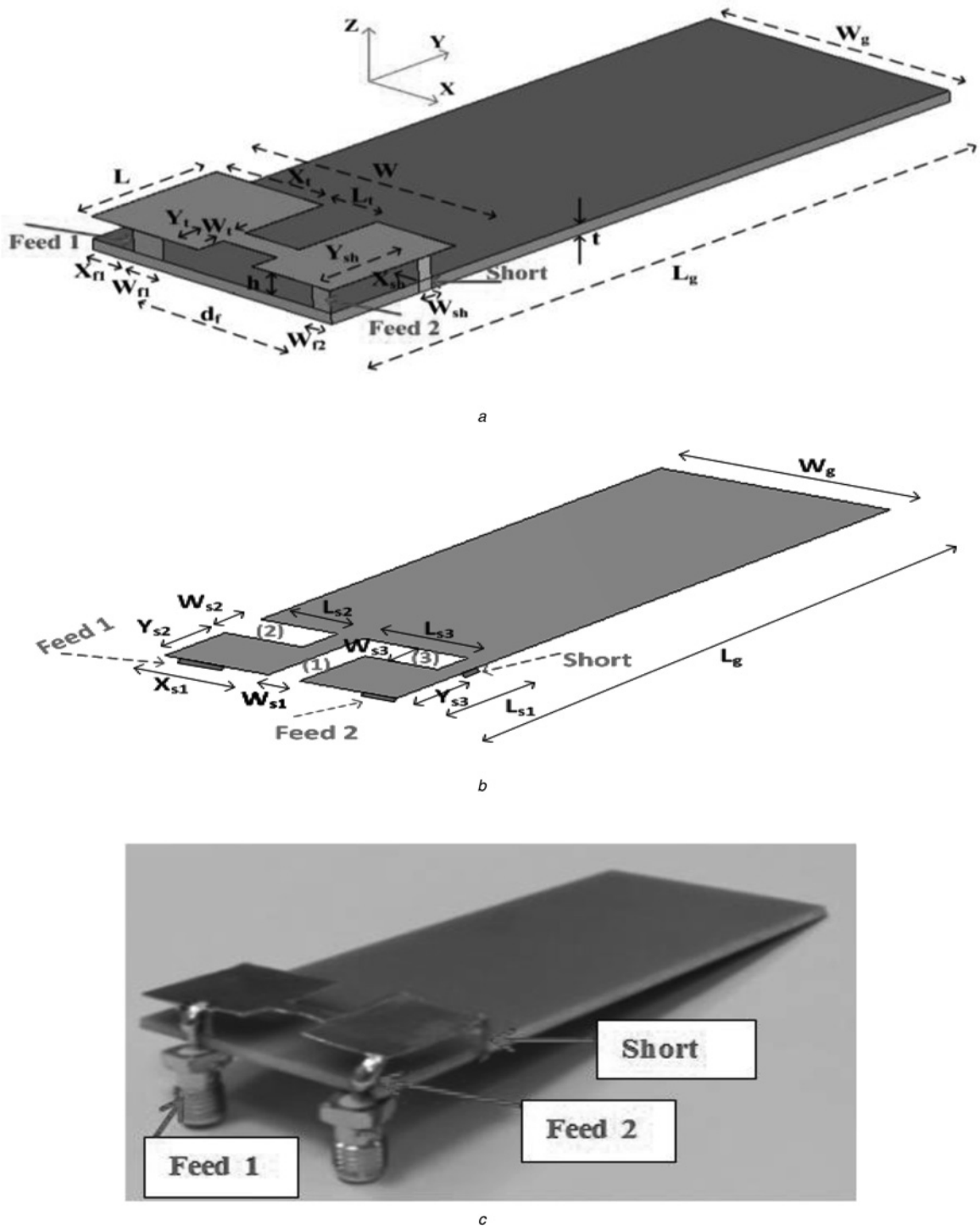

Fig. 4 *Dual coplanar-feed PIFA*

a Structure of dual-coplanar feed PIFA antenna
b Modified ground plane
c Prototype of the proposed antenna

Since both coplanar feeds represent a capacitive coupling element (CCI) (electric source) aligned on the top edge of the chassis (the area of a strong electric field); both feeds excite and share the same characteristic mode at 2.5 GHz [16]. However, an important feature of this feed arrangement is that the geometry of the PIFA and ground plane represent a parallel plate waveguide excited by an electric source (coplanar feed), this waveguide supports transverse electromagnetic mode in *y*-direction – this can be seen from the excited electric and magnetic fields between the top plate and the ground plane as shown in Fig. 3*b* where the arrows on the top plate and ground plane represent the direction of the surface current. Thus, the slot waveguide theory can be employed to analyse and optimise the feed isolation (longitudinal to direction of the surface current), also the radiation can be enhanced if a transverse slot is used [17].

3 Proposed antenna

This work is a continuation of our investigation on the dual-feed PIFA which was originally reported in [18]. Based on the conclusion drawn from the comparative study, a dual

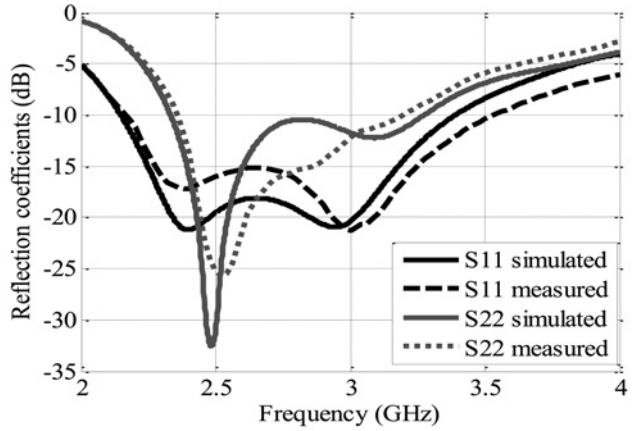

a

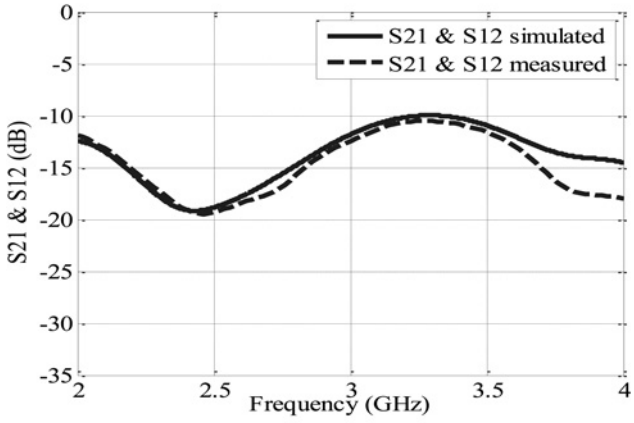

b

Fig. 5 *Measured and simulated S-parameters*

a Reflection coefficients
b Mutual coupling coefficients

coplanar-feed PIFA is proposed and depicted in Fig. 4*a*. The top radiating plate of dimensions $W \times L$ is placed at height h over a PCB substrate of dimensions $L_g \times W_g$. To improve the impedance matching for Feed 2 and to avoid increasing the antenna height (profile), the top plate is modified by creating a small strip with a width W_t, a length L_t, x-position X_t and y-position Y_t. The ground plane has a FR-4 substrate with a thickness $t = 1.5$ mm and a relative permittivity $\varepsilon_r = 4.4$. The radiating plate has three legs, two of them are the feeds, the dimensions of Feed 1 and Feed 2 plates are $W_{f1} \times h$ and $W_{f2} \times h$, respectively. The third leg is the shorting pin with dimensions $W_s \times (h + t)$, x-position X_{sh} and y-position Y_{sh}. Finally, the horizontal distances to Feed 1 and Feed 2 from the side edge are X_{f1} and X_{f2}, respectively.

Fig. 4*b* shows the modified ground plane which contains two main types of slots, an L-shaped slot is formed by Slot 1 and Slot 3 with dimensions $W_{s1} \times L_{s1}$ and $W_{s3} \times L_{s3}$, respectively, this slot represents a band stop resonator to provide the isolation between the feeds. Slot 2 is created with dimensions $W_{s2} \times L_{s2}$ to improve the impedance matching for Feed 1 and it will show later that it also radiate the energy from Feed 1.

4 Simulated and measured results

4.1 Antenna prototype and S-parameters

The simulations are performed using CST Microwave Studio to optimise the antenna parameters for the desired operation band and isolation. A prototype (see Fig. 4*c*) is constructed using the following optimised design parameters (dimensions in [mm]): $L_g = 100$, $W_g = 40$, $L = 16$, $W = 40$, $X_{f1} = 7$, $X_{f2} = 38$, $W_{f1} = 5$, $W_{f2} =$

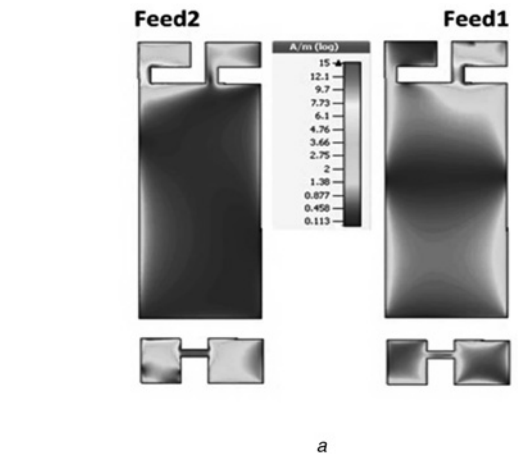

a

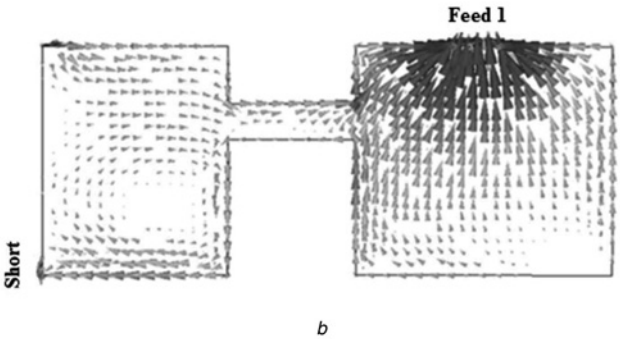

b

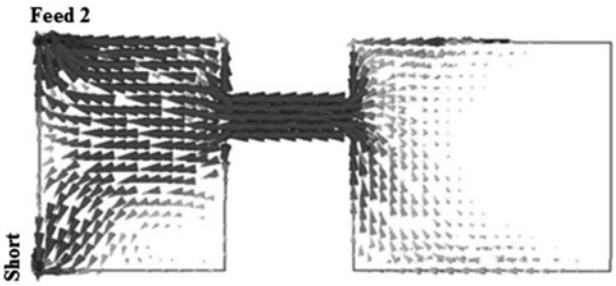

c

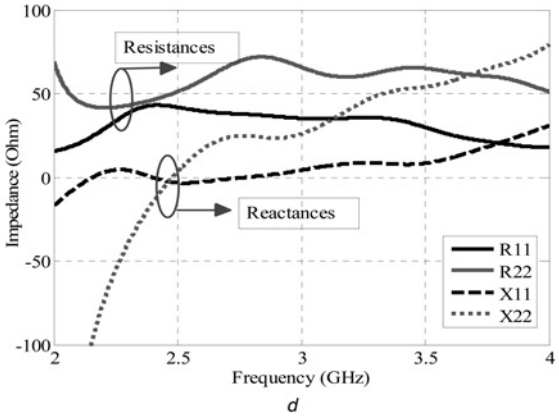

d

Fig. 6 *Current distributions and input impedance characteristics*

a Current distributions at 2.5 GHz
b Direction of currents on the top plate at 2.5 GHz from Feed 1
c Direction of currents on the top plate at 2.5 GHz from Feed 2
d Input impedance as a function of the frequency

IET Microw. Antennas Propag., 2016, Vol. 10, Iss. 2, pp. 152–161

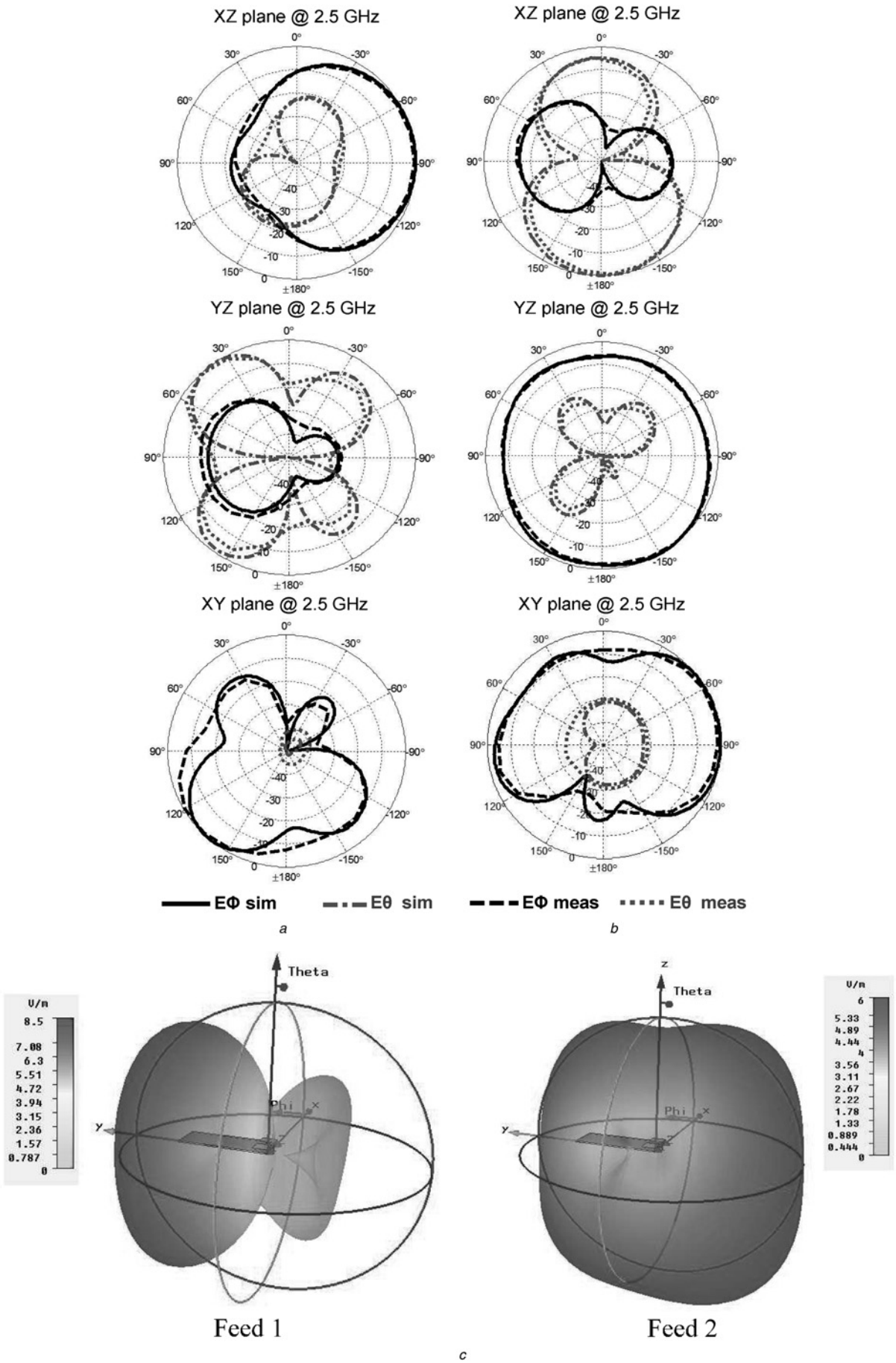

Fig. 7 *Measured and simulated radiation patterns at 2.5 GHz*

a 2D patterns for Feed 1
b 2D pattern for Feed 2
c Simulated 3D radiation patterns for both feeds

2, $d_f = 26$, $X_{sh} = 40$, $Y_{sh} = 15.5$, $W_{sh} = 0.5$, $h = 3$, $t = 1.5$, $L_t = 9$, $W_t = 2.5$, $Y_t = 4$, $X_t = 18$, $X_{s1} = 18$, $W_{s1} = 5$, $L_{s1} = 15$, $W_{s2} = 6$, $L_{s2} = 14$, $Y_{s2} = 9$, $L_{s3} = 18$, $W_{s3} = 6$ and $Y_{s3} = 9$. The simulated and measured S-parameter results are depicted in Fig. 5. They are mostly in a good agreement and a slight discrepancy between them is likely due to the effect of soldering and fabrication errors. The design can cover a wide bandwidth 2.35–3.25 GHz (simulated) with a fractional bandwidth of 32%.

4.2 Current distributions and impedance characteristics

To better understand the achieved results, CST Microwave Studio was used to generate images of the surface current distributions when one feed is excited and the other is terminated with a matched load. Fig. 6*a* shows the current distribution on both the ground plane and the top plate, it can be seen that Feed 1 has a strong current on the open ground plane slot, while Feed 2 has a strong current on the top plate. This means that the antenna fed by Feed 1 is the ground plane slot while the radiation of Feed 2 is mainly from PIFA. Another interesting finding that can give extra evidence on this claim is the current modes on the ground plane. Feed 1 has distributed current mode (usually slot antenna has this kind of mode [19]) while Feed 2 has a localised current mode underneath the top plate (PIFA antenna has this kind of mode [19]). Furthermore, to gain more insight into the achieved results, Figs. 6*b* and *c* show the direction of currents on the top plate fed by Feed 1 and Feed 2 at 2.5 GHz where the arrows represent the direction of the current on the radiator. It can be seen that the two feeds have orthogonal current modes. This leads to the production of both polarisation and pattern diversities.

Furthermore, impedance characteristics can give extra evidence on the operation of the proposed antenna. Fig. 6*d* shows the real and imaginary components of the impedance at feeding Port 1 and Port 2, it shows that Port 2 has a series resonance around 2.5 GHz. This means that Port 2 is connected to a PIFA antenna [20, 21]. On the other hand, Port 1 has a parallel resonance and is linked to a slot antenna (Slot 2) [21]. Moreover, a wide bandwidth is achieved due to the slow change in the impedance around the resonance frequency.

4.3 Far-field radiation patterns

The radiation patterns are produced at 2.5 GHz under the condition that one feed is excited while the other one is terminated with a matched load. The simulated and measured normalised 2D radiation patterns at 2.5 GHz are shown in Figs. 7*a* and *b*. The simulated 3D far field patterns are also presented in Fig. 7*c*. It is apparent that the radiation patterns of the two feeds have pattern and polarisation diversities. These properties provide good antenna diversity in severe fading environments.

5 Parametric study

To gain better insight into the influence of some important design parameters on the frequency response of the reflection coefficients and the mutual coupling coefficients, a parametric study was conducted using CST Microwave Studio. It was done by varying the parameters of interest, while keeping the other design parameters fixed.

5.1 Effect of the open ground plane slot

Fig. 8*a* examines the impact of Slot 2 length (L_{s2}) on the reflection coefficient and impedance matching of Feed 1. It can be seen that S_{11} is sensitive to the length of Slot 2. Furthermore, the study showed that both the length and width of Slot 2 have no effect on Feed 2 response and the isolation level between feeds; because this slot represents a transverse slot in a parallel plate waveguide, which in-turn can help in radiation only [19].

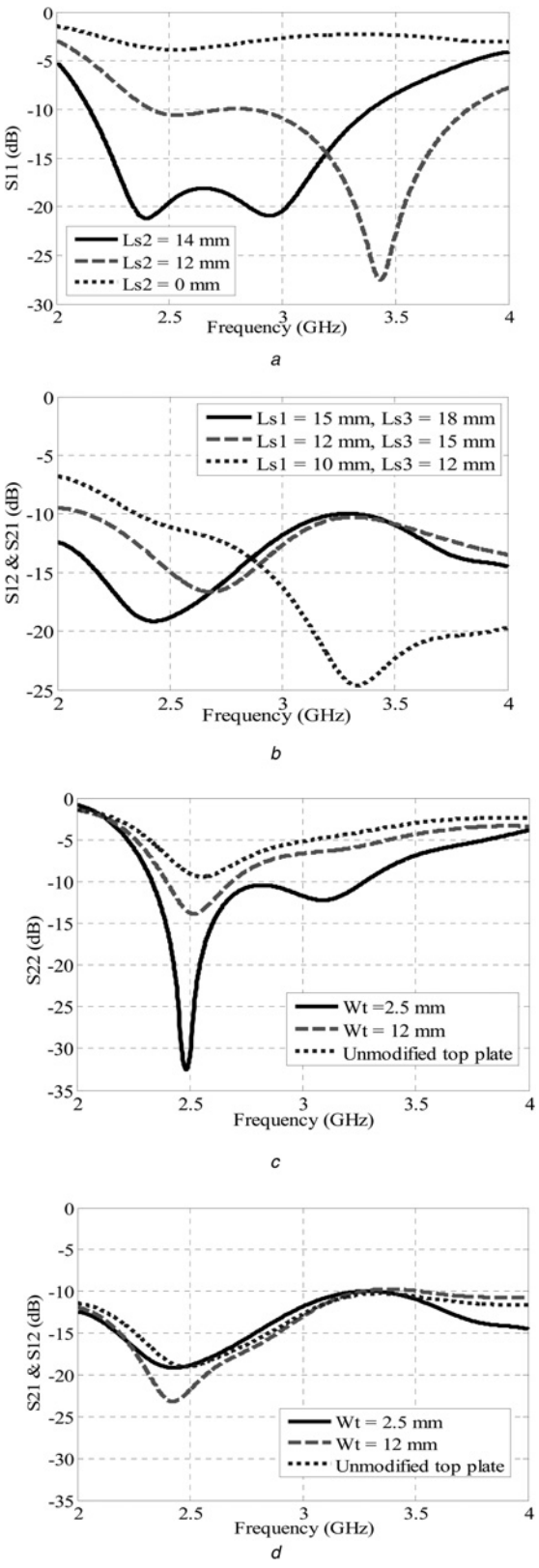

Fig. 8 *Examines the impact of Slot 2 length (L_{s2}) on the reflection coefficient and impedance matching of Feed 1, the influence of the L-shaped slot lengths on the mutual coupling coefficients (S_{21} and S_{12}) and the effect of the modified top plate on impedance matching of Feed 2*

a Effect of Slot 2 with different lengths on S_{11}
b Effect of different L-slot lengths on the mutual coupling coefficient
c Effect of top plate strip width on the reflection coefficient of Feed 2
d Effect of top plate strip width on the mutual coupling coefficient

IET Microw. Antennas Propag., 2016, Vol. 10, Iss. 2, pp. 152–161

5.2 Effect of the L-shaped slot (slot 1 and slot 3)

Fig. 8*b* shows the influence of the L-shaped slot lengths on the mutual coupling coefficients (S_{21} and S_{12}). It can be observed as the lengths increased; the stop band frequency is decreased (dips on the curves). This can be interpreted from the theory of the transmission line resonators [22], the L-shaped slot represents a band stop transmission resonator formed from Slot 1 that represents a shunt open-circuit quarter wavelength stub, and Slot 3 which works as a series short-circuit quarter wavelength stub. Although the isolation can be improved, the creation of this slot structure has a negative effect on the level of matching of Feed 2. This is because the position of the slot is located between Feed 2 and the shorting pin.

5.3 Effect of the top plate strip

It can be seen from Fig. 8*c*, the effect of varying the width of the top plate strip is on the level of the impedance matching of Feed 2. This can be interpreted as a simple matching circuit is formed from a series inductance (small width strip) and a shunt capacitance (capacitance between the left-hand side of the top plate and the ground plane) [23]. There is no need to increase the antenna profile, thus the proposed antenna has the lowest profile compared the other designs in [13–15].

A question now is how much this strip will affect the feed isolation. To answer this question, a further parametric study has been done on the parameters of the strip; such as the strip width, strip position and strip length. The results demonstrate that the top plate strip affects only the level of matching of Feed 2. Fig. 8*d* shows that the width of the strip has little effect on the level of isolation. This leads to the conclusion that the small strip on the top plate is to improve the impedance match, not the isolation, thus it is different from the neutralisation line in [24].

6 Diversity and MIMO performance

The diversity characteristics and MIMO performance of the proposed antenna are simulated, measured, and evaluated in free space. Parameters such as ECC, antenna branch power ratio in terms of the MEG ratio, the total efficiencies and the diversity gain are presented in this section.

6.1 Mean effective gain and envelope correlation coefficient

The amount of reduction in signal fading (diversity gain) strongly depends on two criterions that should be satisfied [5]. The first one is the ECC which is a measure of the discrepancy between received signals; and the second one is the branch power ratio which is a measure of the power difference at the two ports/feeds. These two diversity conditions are summarised as follows [5]

$$\rho_e \leq 0.5, \quad k = \left|\frac{\mathrm{MEG}_1}{\mathrm{MEG}_2}\right| \cong 0\,\mathrm{dB} \tag{1}$$

where ρ_e is the ECC, k is the branch power ratio and MEG is the mean effective gain.

MEG for an antenna is defined as the ratio of the mean received power to the total mean incident power. It depends on several parameters such as the radiation power pattern, total antenna efficiency and the propagation characteristics of mobile communication environments [25]. It can be calculated using the

Table 1 Diversity parameters in different propagation environments

Environment	Gaussian/indoor	Gaussian/outdoor
statistical parameters	$\sigma_V = \sigma_H = 30°$ $m_V = m_H = 20°$ XPR = 1 dB	$\sigma_V = \sigma_H = 15°$ $m_V = m_H = 10°$ XPR = 6 dB
MEG_1, dB	−3.23	−6.12
MEG_2, dB	−3.33	−5.89
$\lvert\mathrm{MEG}_1/\mathrm{MEG}_2\rvert$ dB	0.1	0.27

m_V and m_H are mean elevation angles of the vertical and horizontal polarised wave distribution, while σ_V and σ_H are the standard deviation of vertical and horizontal polarised wave distribution [26]

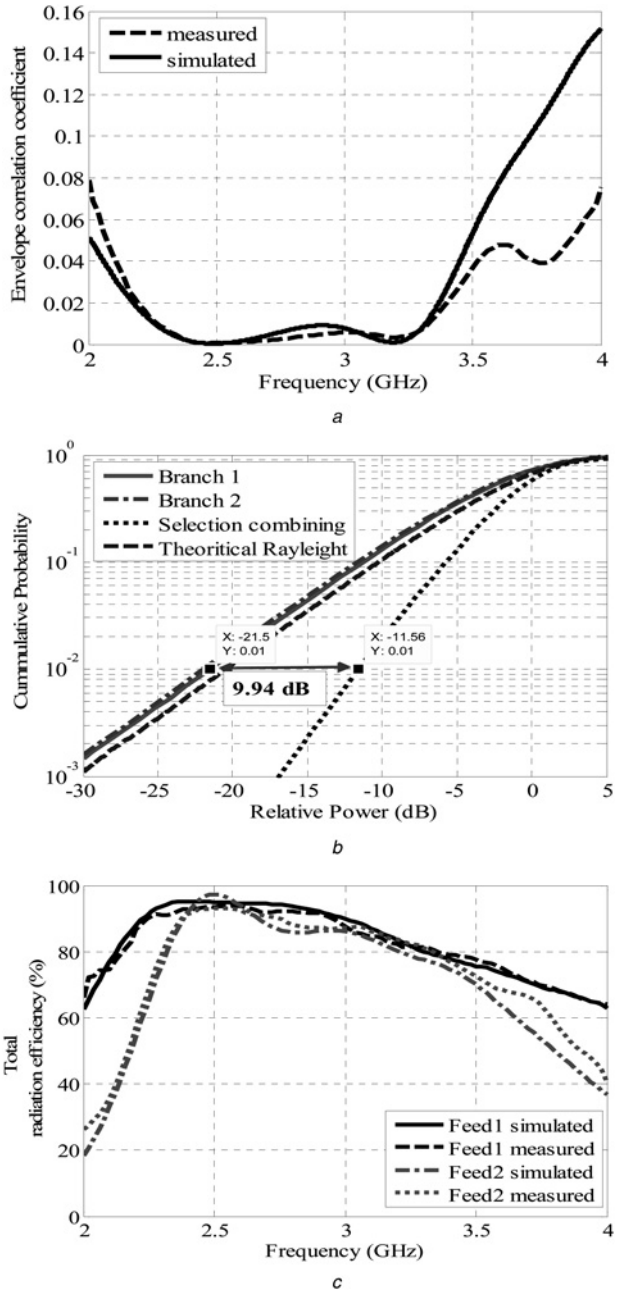

Fig. 9 *The diversity performance parameters*

a Envelope correlation coefficient
b CDF functions and apparent diversity gain
c Total radiation efficiency

Table 2 Comparison of the proposed design with previous works

Ref	Plate, mm × mm	Height, mm	Feed arrangement	Diversity scheme	Frequency bandwidth, GHz	Modified ground, mm^2	DG, dB
[13]	20 × 40	10	orthogonal	pattern and polarisation	simulated (2.4–2.6) measured (2.35-2.7)	772	10.1
[14]	20 × 40	5	parallel	pattern	simulated (2.4–2.47) measured (2.3–2.6)	711	9.95
[15]	20 × 40	10	parallel	pattern	simulated (2.4–2.6) measured (2.35–2.7)	644	9
[this design]	16 × 40	3	coplanar	pattern and polarisation	simulated (2.35–3.2) measured (2.35–3.2)	256	9.95

following equation

$$\mathrm{MEG} = \int_0^{2\pi}\int_0^{\pi}\left[\frac{\mathrm{XPR}}{\mathrm{XPR}+1}G_\theta(\theta,\varphi)\cdot P_\theta(\theta,\varphi) + \frac{1}{\mathrm{XPR}+1}G\varphi(\theta,\varphi)\cdot P_\varphi(\theta,\varphi)\right]\sin(\theta)\cdot \mathrm{d}\theta\cdot \mathrm{d}\varphi \tag{2}$$

where XPR is the cross polarisation ratio of average power of incident field in different polarisation states, G_θ and G_Φ are θ and Φ components of antenna power gain, and P_θ and P_Φ represent θ and Φ components of angular density functions of the incident power, respectively. All these parameters are strongly dependent on the statistical and propagation characteristics of communication environments.

Several propagation scenarios have been discussed (indoor, outdoor and isotropic) based on statistical models such as Gaussian, Laplacian and uniform distribution models. Here, the value of branch power ratio is calculated in Gaussian environment with typical statistical values for indoor, outdoor and isotropic environment [26]. Table 1 shows the calculated values from CST simulation using (2).

The calculated data in Table 1 show that the MEG ratio in the isotropic environment meets the branch power ratio requirement in (1). Moreover, the calculated values over the defined Gaussian model in both indoor and urban outdoor environments have satisfied the acceptable diversity criteria of branch power ratio (<3 dB [5]).

On the other hand, ECC can be calculated using S-parameters and radiation efficiency if the antenna loss is not small [27].

$$\rho_e = \left|\frac{\left|(S_{11}^*S_{12}+S_{22}S_{21}^*)\right|}{\left|(1-|S_{11}|^2-|S_{21}|^2)\cdot(1-|S_{22}|^2-|S_{12}|^2)\cdot\eta_{\mathrm{rad1}}\cdot\eta_{\mathrm{rad2}}\right|^{0.5}}\right|^2 \tag{3}$$

where S_{ij}'s are the S-parameters of the dual-feed antenna, * denotes the complex conjugate operator, |.| is the magnitude operator, η_{rad}'s the radiation efficiencies and ρ_e is the ECC.

On the basis of measured and simulated data, ECC is calculated and presented in Fig. 9*a*. It shows that the simulated and measured values are in a good agreement; also the values of ECC are <0.02 within the whole operation band. Based on (1), ECC satisfies the condition and this is another good metric for MIMO system.

6.2 Diversity gain

The diversity gain is the most important performance parameter of MIMO and diversity antennas. Normally, it is defined as [25]

$$G_{\mathrm{div}} = \frac{P_{\mathrm{div}}}{P_{\mathrm{Branch}}}@\ \text{Specific CDF value} \tag{4}$$

where P_{div} is the power level after applying diversity combining technique and P_{branch} is the power level of the reference branch. Both values should be taken at the same level of cumulative distribution function (CDF).

The diversity gain measurement was carried out inside our reverberation chamber. Based on the DG definition above, it is obtained and by employing selective combining technique and Fig. 9*b* shows that the apparent diversity gain at 0.01 CDF level is about 9.95 dB. This demonstrates that the proposed antenna can provide a high diversity gain as we can also see from Table 2. Furthermore, Table 2 compares the top plate dimensions, antenna profile, modified ground plane area, feed arrangement, frequency bandwidth and diversity gain of the proposed design with some recently published results. It shows that the proposed design has achieved excellent performance with the lowest profile, smallest modified ground plane area (256 mm^2) and largest bandwidth. Thus, the antenna is a good candidate for modern handset applications.

6.3 Total radiation efficiency

As the design represents a multi-port antenna, it is important to calculate the total radiation efficiency using

$$\eta_{\mathrm{tot}} = \eta_{\mathrm{rad}}\left(1-|S_{11}|^2-|S_{12}|^2\right) \tag{5}$$

where η_{rad} is the radiation efficiency, S_{11} is the reflection coefficient of the antenna element, while S_{12} is the transmission coefficient between two antenna elements.

The same collected data from the diversity gain measurement was used in calculating the total efficiencies. The simulated and measured total efficiencies are depicted in Fig. 9*c*. It shows that the proposed antenna has high total radiation efficiency (>80%) over the frequency band of interest.

7 Conclusions

In this work, a new wideband, low profile (height = 3 mm) dual-coplanar-feed PIFA antenna has been presented as a diversity and MIMO antenna for wireless applications over the frequency band 2.35–3.25 GHz. The key of this design lies in the use of a new feed arrangement that exhibits a lower mutual coupling level compared with other feed arrangements. Both pattern and polarisation diversities have been achieved by exciting two orthogonal modes. Feed 1 radiation is mainly from the open ground plane slot, while Feed 2 radiation comes from PIFA loop mode. The feed isolation has been achieved via the L-shaped ground plane slot. Both simulated and measured results have been presented in a good agreement. The results also have showed that this antenna has a good diversity performance across the whole operational bandwidth.

It should be pointed out that the frequency band can be easily scaled up or down to cover the desired frequencies using the same design idea. It is noted that the width of the mobile for this investigation is just 40 mm while most of the latest smart phones have a width of 70 mm. As an example: if we increase the width to 55 mm (a scaling factor of 1.33), the design can cover about 1 GHz 6-dB bandwidth (1.70 to 2.70 GHz).

8 References

1 Foschini, G., Gans, M.: 'On limits of wireless communications in a fading environment when using multiple antennas', *Bell Labs Tech. J.*, 1996, **1**, (2), pp. 41–59
2 Zhang, S., Lau, K.B., Tan, Y., *et al.*: 'Mutual coupling reduction of two PIFAs with a T-shape slot impedance transformer for MIMO mobile terminals', *IEEE Trans. Antennas Propag.*, 2012, **60**, (3), pp. 1521–1531
3 Dietrich, B.C., Dietze, K. Jr., *et al.*: 'Spatial, polarization and pattern diversity for wireless handheld terminals', *IEEE Trans. Antennas Propag.*, 2001, **49**, (9), pp. 1271–1281
4 Caimi, F., Mongomery, M.: 'Isolated mode antenna technology (IMAT)' (SkyCross, Inc, 2008), pp. 1521–1531
5 Vaughan, G.R., Anderson, B.J.: 'Antenna diversity in mobile communications', *IEEE Trans. Veh. Technol.*, 1987, **36**, (4), pp. 149–172
6 Anderson, J., Rasmussen, H.: 'Decoupling and descattering networks for antennas', *IEEE Trans. Antennas Propag.*, 1976, **24**, (6), pp. 841–846
7 Dassche, S., Rodriguez, J., Jofre, L., *et al.*: 'Decoupling of a two-element switched dual band patch antenna for optimum MIMO capacity'. Proc. Third Europian Conf. on Antennas and Propagation (EuCAP 2009), Germany, March 2009, pp. 1114–1118
8 Diallo, A., Luxey, C., Thuc, L., *et al.*: 'Enhanced two-antenna structures for universal mobile telecommunications system diversity terminals', *IET Antennas Microw. Propag.*, 2008, **2**, (1), pp. 93–101
9 Holopainen, J., Kivekas, O., Icheln, C., *et al.*: 'Internal broadband antennas for digital television receiver in mobile terminals', *IEEE Trans. Antennas Propag.*, 2010, **58**, (10), pp. 3363–3374
10 Yuk-C, C., Cheng, C.H., Murch, R.D., *et al.*: 'Reduction of mutual coupling between closely-packed antenna elements', *IEEE Trans. Antennas Propag.*, 2007, **55**, (6), pp. 1732–1738
11 Yao, Y., Wang, X., Chen, X., *et al.*: 'Novel diversity/MIMO PIFA antenna with broadband circular polarization for multimode satellite navigation', *IEEE Antennas Wirel. Propag. Lett.*, 2012, **11**, pp. 65–68
12 Chen, C.S., Wang, S.Y., Chung, J-S.: 'A decoupling technique for increasing the port isolation between two strongly coupled antennas', *IEEE Trans. Antennas Propag.*, 2008, **56**, (12), pp. 3650–3658
13 Chattha, T.H., Huang, Y., Boyes, J.S.: 'Polarization and pattern diversity-based dual-feed planar inverted-F antenna', *IEEE Trans. Antennas Propag.*, 2012, **60**, (3), pp. 1532–1539
14 Chattha, T.H., Huang, Y.: 'Low profile dual-feed planar inverted-F antenna for wireless LAN applications', *Microw. Opt. Technol. Lett.*, 2011, **53**, pp. 1382–1386
15 Chattha, T.H., Huang, Y., Zhu, X.: 'Dual-feed PIFA diversity antenna for wireless applications', *Electron. Lett.*, 2010, **46**, (3), pp. 189–190
16 Rahola, J., Ollikainen, J.: 'Optimal antenna placement for mobile terminals using charactristic mode analysis'. Proc. First European Conf. on Antennas and Propagation (EUCAP 2006), France, November 2006, pp. 1–6
17 Silver, S.: 'Microwave antenna theory and design' (McGraw-Hill, 1949)
18 Aljaafreh, S.S., Huang, Y., Xing, L.: 'A new dual feed PIFA diversity antenna'. Proc. European Conf. on Antenna and Propagation (EuCAP 2014), Netherlands, April 2014, pp. 1–4
19 Hui, L., Tan, Y., Lau, K.B., *et al.*: 'Characteristic mode based tradeoff analysis of antenna-chassis interactions for multiple antenna terminals', *IEEE Trans. Antennas Propag.*, 2012, **60**, (2), pp. 490–502
20 Schulteis, S., Sorgel, W., Waldschmidt, C., *et al.*: 'A small planar inverted f antenna with capacitive and inductive loading'. IEEE Antennas, Propagation Society Int. Symp., 2004, no. 4, pp. 4148–4151
21 Binboga, S.Y.: 'Design of ultra wideband antenna matching networks: via simplified real frequency technique' (Springer, 2008)
22 Pozar, M.D.: 'Microwave engineering' (John Wiley & Sons, 1998)
23 Young, H.P.: 'Electronic communications techniques' (Prentice Hall, 2003)
24 Diallo, A., Luxey, C., Thuc, L., *et al.*: 'Study and reduction of the mutual coupling between two mobile phone PIFAs operating in the DCS 1800 and UMTS bands', *IEEE Trans. Antennas Propag.*, 2006, **54**, (11), pp. 3063–3074
25 Taga, T.: 'Analysis for mean effective gain of mobile antennas in land mobile radio environments', *IEEE Trans. Veh. Technol.*, 1990, **39**, (2), pp. 117–131
26 Ding, Y., Zhengwei, D., Gong, K., *et al.*: 'A novel dual-band printed diversity antenna for mobile terminals', *IEEE Trans. Antennas Propag.*, 2007, **55**, (7), pp. 2088–2096
27 Poul, H.: 'The significance of radiation efficiencies when using S-parameters to calculate the received signal correlation from two antennas', *IEEE Antennas Wirel. Propag. Lett.*, 2005, **4**, (1), pp. 97–99